Paper 27

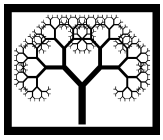

Proceedings of the Eighth International Conference on Engineering Computational Technology, B.H.V. Topping, (Editor), Civil-Comp Press, Stirlingshire, Scotland

The Effect of Fibre Reinforced Polymer Sizes on Debonding when Retrofitting Reinforced Concrete Beams

Y.H. Kim, Y.S. Shin and H.S. Kim
Department of Architectural Engineering
EWHA Womans University, Seoul, South Korea

Abstract

This paper presents analytical studies for the evaluation of the structural performance of reinforced concrete (RC) beams with externally attached fibre reinforced polymers (FRPs) of different sizes. Towards this goal, an analytical modelling approach is developed to simulate the structural behaviour of RC beams of different lengths, widths and numbers of FRP layers. Commercial finite element (FE) software, ABAQUS version 6.10-3, is used for the FE modelling. The analytical results show that the proposed modelling approach can be used to not only simulate structural behaviour of concrete beams retrofitted with FRPs, but also to investigate the effect of FRP sizes on debonding in FRPs.

Keywords: fibre reinforced polymer, carbon fibre, debonding, finite element analysis, reinforced concrete beam.

1 Introduction

FRPs are used for strengthening structural members such as beams, slabs and columns due to its wide range of application and high strength. For instance, flexural and shear capacity of beams can be increased by attaching fibre reinforced polymers (FRPs) on the flexural and side surfaces of the beams. Teng et al.[6] identify seven main categories of failure modes for RC beams retrofitted with FRPs: (a) flexural failure by FRP rupture, (b) flexural failure by crushing of the compressive concrete, (c) shear failure, (d) concrete cover separation, (e) plate end interfacial debonding, (f) intermediate flexural crack-induced debonding, and (g) intermediate flexural shear crack- induced failure. Since the debonding in FRP is critical issue for beams strengthened using FRPs, experimental and numerical studies for investigating debonding in FRPs used to strengthen concrete beams have been reported [1-12]. Especially, Kamel et al. [10] perform regression analyses based on experimental

results from the literature to develop numerical models capable of predicting the effective bond lengths and bond capacities of FRP sheets bonded to concrete. Furthermore, Teng et al. [12] make use of a realistic bi-linear local bond-slip law to develop an analytical solution for the debonding process in an FRP-to-concrete bonded joint model. Also, formulations for FRPs are proposed to predict the debonding strength considering the effect of elastic modulus, thickness, and the size of FRPs. Nadia [13] performs experimental and analytical studies to investigate debonding in hybrid FRPs where carbon and glass fibre FRPs are combined. In this paper, debonding strength is calculated using previously developed numerical models such as shear capacity model, and compared to debonding strength adopted from the experimental measurements. The latter value is applied to the finite element (FE) model and the analytical results are in good agreement with the experiments.
In this study, analytical studies are performed to investigate the effect of CFRP sizes on the structural behaviour of RC beams externally attached with carbon fibre reinforced polymers (CFRP). FE modelling methods are developed to simulate the overall behaviour of RC beams including material nonlinearity of the concrete and the debonding of the CFRPs.

2 Modelling method

2.1 Modelling plan

In order to investigate the effect of FRP sizes on the structural performance of RC beams externally attached with FRPs, variables are determined as shown in Table 1. The beams are strengthened with two, three, or four layers of CFRPs with different FRP width and length. Type A models have the same CFRP length of 1800mm, while B and C types are designed such that the length of each CFRP layer is different by 300mm. CFRP width are varied as 200mm, 300mm, and 400mm. Also, the 2A200U model is strengthened with a U-strap for shear strengthening as well as two layers of CFRPs on the tension side.

The simulation, is planned such that reinforced concrete beams (200x250x3200mm) are subjected to four point-bending with simply supported condition. All the beams are strengthened using CFRP sheet in the tensional surface only except for control beam. For the steel reinforcement, two D13 (diameter=13mm) reinforcing bars are placed on the flexural side of the concrete beams with a cover thickness of 30mm. Also, as shear reinforcement, D10 (diameter=10mm) bars are placed in order to prevent shear failure of the beams. The geometry, reinforced arrangement, loads, as well as support arrangements are illustrated in Figure 1.

Models	FRPs length(mm)				FRPs width (mm)
	1layer	2layer	3layer	4layer	
4A200	1800	1800	1800	1800	200
4B200	1800	1500	1200	900	
4C200	2100	1800	1500	1200	
3A200	1800	1800	1800	-	
3B200	1800	1500	1200	-	
2A200	1800	1800	-	-	
2B200	1800	1500	-	-	
2A200U	1800	1800	-	-	U-strap
2A300	1800	1800	-	-	300
2A400	1800	1800	-	-	400
CONT.	-				

Table 1: Details of the test variables

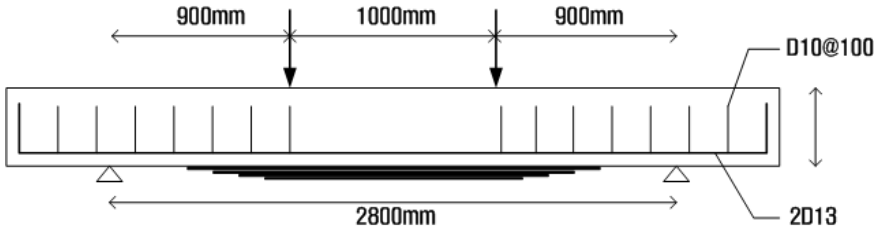

Figure 1: Model illustration

2.2 FE models

For the analysis, FE models are generated as illustrated in Figure 2. The model includes four different parts; concrete, steel reinforcement, epoxy, and FRP composite. The types of elements used for each part are listed in Table 2. Concrete and FRP elements are generated using three-dimensional continuum brick elements. For epoxy, cohesive elements are used with elastic-traction material behaviour to consider debonding. In the epoxy model, damage initiation criteria is also included, which is obtained using an existing formulation for debonding strength [4-12] and the small beam test results [13]. The formulation is able to capture the effect of stiffness and dimensions of the CFRPs on the interfacial stresses between the concrete and CFRPs, and works well with multi-layered FRPs. To consider material nonlinearity, existing experimental data from concrete compressive and tensile tests are adopted for the concrete material model. For reinforcing bars, stirrup, and CFRPs, a linear elastic material model is used based on the assumption such that steel bars will not reach yield level under the loading and the CFRP does not show plastic behaviour from its material tests. Mechanical material properties of the CFRPs are obtained from coupon tensile tests [13]. The material properties of concrete, reinforcing bars, and CFRPs are listed in Table 3.

In addition, the loading is applied as a form of displacement control and simply supported boundary conditions are prescribed in the model. The static analysis is performed with geometrical nonlinearity.

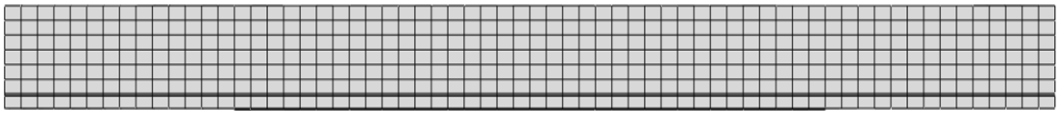

Figure 2: The finite element model

Part	Element type		Material
Concrete	3D continuum brick	C3D8R	Elastic and Concrete Smeared Cracking model
Steel reinforcement	3D Truss	T3D2	Elastic
Epoxy	Cohesive	COH3D8	Elastic Traction (shear capacity based model)
FRP composite	3D continuum brick	C3D8R	Elastic

Table 2: Element types and materials model

Material	Elastic modulus	Compressive strength	Tensile strength
Concrete	23.7 GPa	30 MPa	3 MPa
D10	204 GPa	-	450MPa
D13	226 GPa	-	450MPa
CFRP	230 GPa	-	1300MPa

Table 3: Material properties

3 Analytical results

3.1 Effect of number of CFRP layers

3.1.1 Load-displacement relationships

Load-displacement relationships obtained from the analysis is illustrated in Figure 3. In the figure, load-displacement relationships of RC beams strengthened by two, three and four layers of CFRPs are compared. The stiffness of the beams strengthened by CFRPs increases with number of CFRP layers, however, the beams with the larger number of CFRP layers show the earlier failures caused by debonding in the CFRPs. Therefore, even if the larger numbers of CFRPs are used for strengthening, the capacity of the FRPs is not fully utilized at the time of beam failure. Regarding the load carrying capacity, 4A200 and 3A200 models are the last to fail at 185kN. Model 2A200 failed at 189kN and has a higher peak load than the 3A200 model and the 4A200 model. The control beam has the lowest maximum load and fails when the load reaches 114kN. Analysis results have shown that the

CFRP strengthens concrete beam, and maximum loads are increased by approximately 62% compared to the control beam. Also, the maximum deflections of all the strengthened beams are reduced under the same load compared with the control beam. However, it is noted that the control beam is more ductile than beams strengthened using CFRPs.

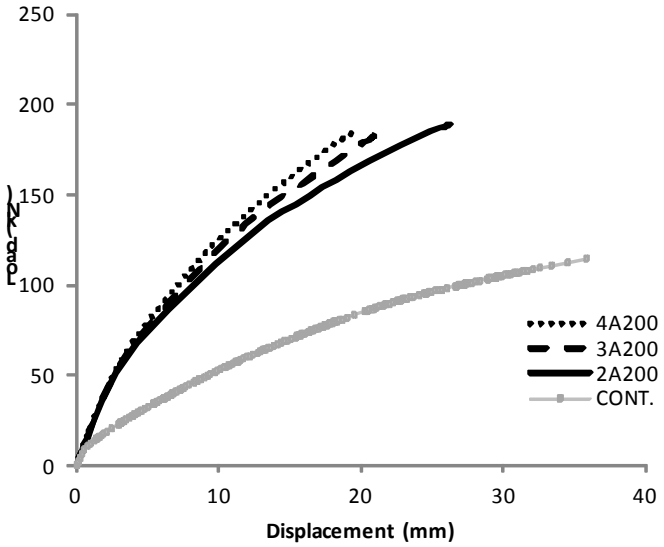

Figure 3: Comparison of load-displacement relationships of beams retrofitted with FRPs and CONT.

3.1.2 Deformation configuration with stress contour

The predicted deformation shapes of the control beam and the beam strengthened with two layers of CFRPs are illustrated as Figure 4. For the case of the 2A200 model, a higher peak load than the control beam are obtained as seen in Figure 2, however, deformation of the strengthened beam is decreased at the time of beam failure compared with the control beam, which indicates that the FRP can significantly improve the strengthening of the RC beam.

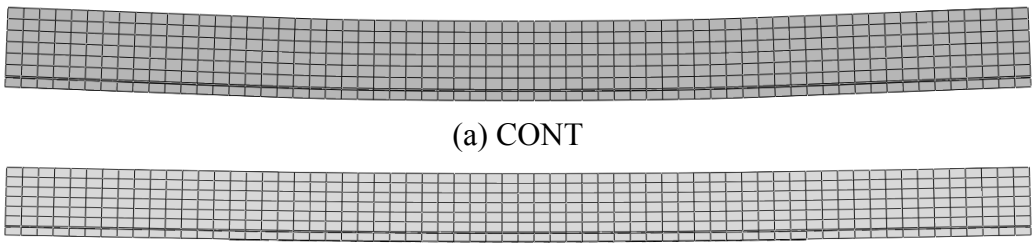

(a) CONT

(b) 2A200

Figure4: Comparison of deformation configurations of (a) the control beam and (b) the beam strengthened with two layers of CFRPs

3.2 Effect of FRP length

3.1.2 Load-displacement relationships

Load-displacement relationships depending on CFRP length are predicted from the analytical model as illustrated in Figures 5 to 7. Regardless of numbers of the CFRP layers, about 2.6-5.5% of the maximum loads are increased when the beams are strengthened with tapered CFRPs, with respect to non-tapered CFRPs. It is interesting to note that the effect of tapered CFRPs on maximum load capacity decreases when the numbers of CFRP layers are four. As seen from Figure 5, the RC beams strengthened with four layers of CFRPs, the strengthening effect is not significantly dependent on the length of CFRP even though the length of the shortest CFRP is longer than 60% of the beam length. However, the beams with tapered layers of CFRP show higher peak loads than the beams with non-tapered layers of CFRPs, as the debonding failure is delayed at the end of the tapered CFRP laminates. Between the beams with tapered CFRPs, the longer CFRP length delays the more the beam failure. For example, the 4C200 using four layers of CFRPs of lengths of 2100, 1800, 1500 and 1200 mm presents a slightly higher peak load than the 4B200 using the same number of CFRP layers of lengths that are 1800, 1500, 1200 and 900mm.

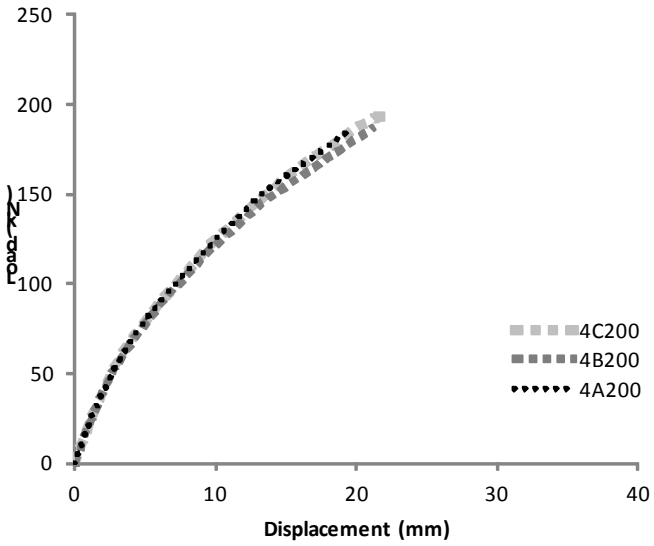

Figure 5: Load-displacement relationships for beams retrofitted with four layers of CFRPs

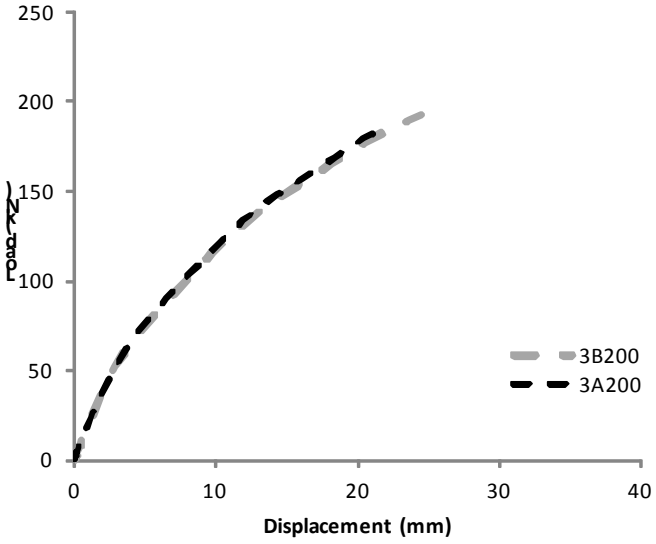

Figure 6: Load-displacement relationships for beams retrofitted with three layers of CFRPs

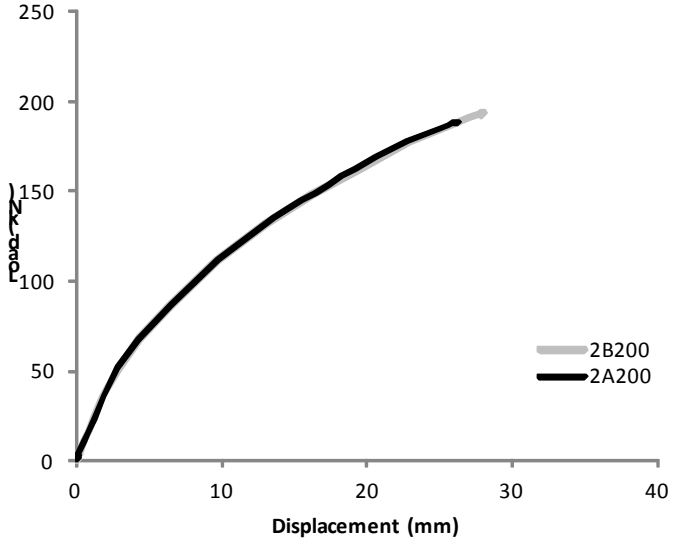

Figure 7: Load-displacement relationships for beams retrofitted with two layers of CFRPs

3.2.2 Stress contours on bottom surface of the beams strengthened with various length and layers of CFRPs

Analytical results of the maximum principal stresses are presented in Figures 8 to 10. Generally, lower stress concentration is observed from the beams strengthened with tapered layers of CFRPs compared with the beams with non-tapered layers of CFRPs. Especially, when four layers of CFRP with lengths of 1800, 1500, 1200 and 900mm are attached at the bottom of beam (Figure 8(b)), the distribution of stresses

for the FRP is different from the 4C200 (Figure 8(c)) and 4A200 (Figure 8(a)), even the maximum load capacity is larger than the other two cases. Therefore, it can be said that the tapered layers of FRP strengthening reduces stress concentrations on FRPs which can delays failure as a result of debonding in the FRPs.

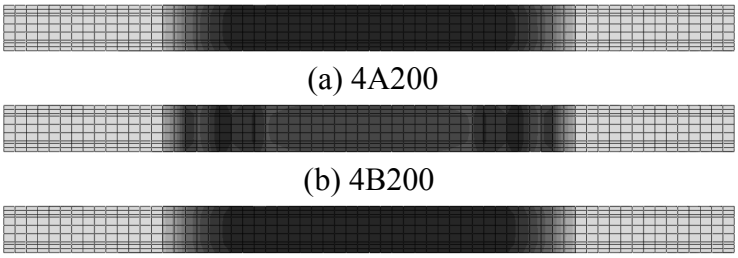

(a) 4A200

(b) 4B200

(c) 4C200

Figure 8: Stress contour of the bottom surface of the beams strengthened with four layers of FRPs

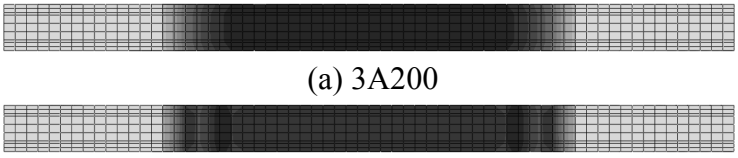

(a) 3A200

(b) 3B200

Figure 9: Stress contour of the bottom surface of the beams strengthened with three layers of FRPs

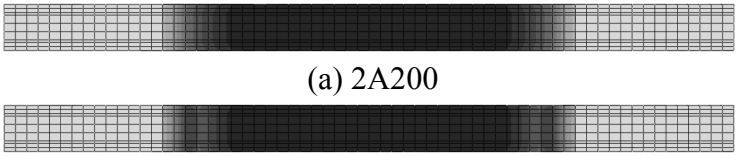

(a) 2A200

(b) 2B200

Figure 10: Stress contour of the bottom surface of the beams strengthened with two layers of FRPs

3.3 Effect of CFRP width

3.3.1 Load-displacement relationships

The effect of the CFRP widths on load-displacement relationships are presented in Figure 11. There is no significant difference of slopes of the load-displacement curves, but the maximum load capacity is obtained from the beam strengthened in

shear using a U-strap as the failure is delayed the most. It is well known that U shaped straps can be bonded to the ends of FRPs to delay and prevent plate end debonding failures, as predicted from the analysis. As seen in Figure 10, the 2A200 model fails at 189kN, while the 2A200U model fails when the load reaches 207kN. Therefore, the U shaped straps are able to increase the maximum load by 9.5% compared to the non-shear strengthened beams. However, increasing the width of the CFRP does not increase load capacity, because concrete cover separation occurs along the location of reinforcing steel bars as a result of the high interfacial stresses between concrete and CFRPs. Therefore, model 2A400 has the lowest maximum load and fails when the load reaches 95kN and the model 2A300 fails at 138kN.

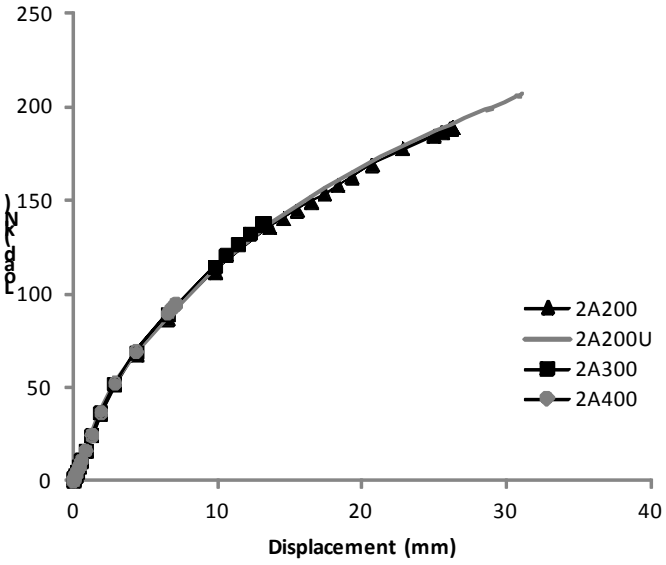

Figure 11: Load-displacement relationships of beams with various widths of CFRPs

3.2.2 Stress contours on side and bottom surfaces of the beams strengthened with various widths of CFRPs

Deformation configurations with maximum principal stresses of the beams strengthened with various widths of CFRPs are presented in Figures 12(a) to (d). It can be seen that stresses at the end of the CFRPs are reduced as a U strap is added to the beam. The beams with a CFRP width of 300mm and 400mm does not influence the stresses on the bottom surfaces, however the stresses on the side area increased as the concrete cover separation are leads to high interfacial stresses between the concrete and FRPs. Therefore, FRP can strengthen the concrete beam effectively when the FRP width is less than the width of beam.

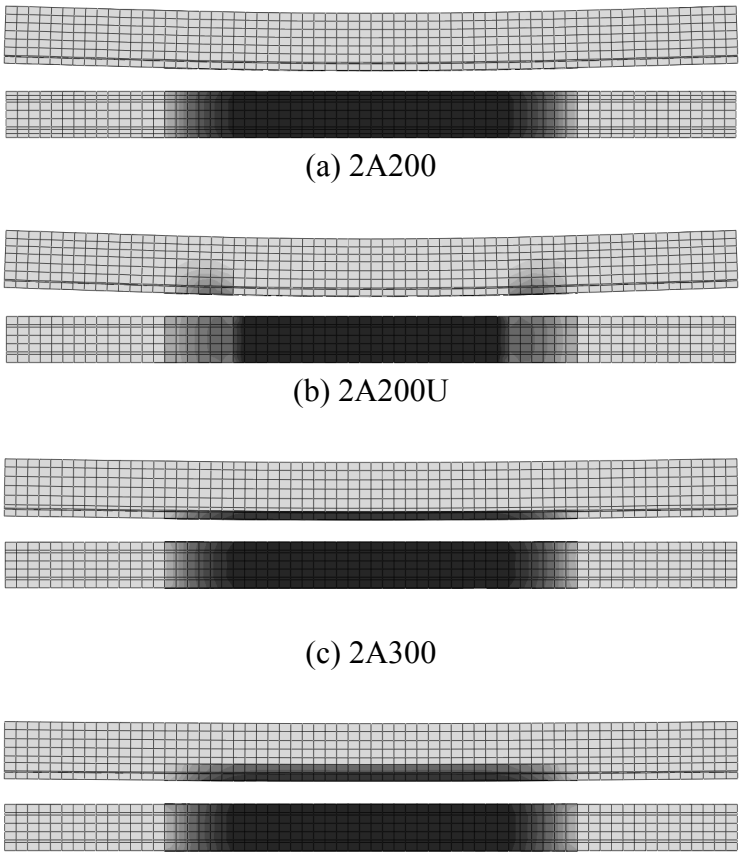

(a) 2A200

(b) 2A200U

(c) 2A300

(d) 2A400

Figure 12: Stress contour of side and bottom surfaces of the beams strengthened with two layers of CFRPs which width of (a) 200mm, (b) 200mm with U strap (c) 300mm, and (d) 400mm. (Deformation scale : 1.0)

4 Conclusion

In this paper, the analysis of reinforced concrete beams strengthened by CFRPs has been performed. Based on the results, following conclusions can be drawn:

1) CFRP can significantly improve the load capacity of an RC beam. The stiffness of the beams strengthened with CFRPs increases with the increase of CFRP thickness, however, beams strengthened with four or more layers of CFRPs show earlier failures caused by debonding in the FRPs.
2) The effect of the CFRP length on the load-displacement relationship is not significant if the length of the first layer of CFRP reaches 60% of beam span length. When multiple layers of CFRPs are used for strengthening, beams with the tapered layers of CFRP are able to avoid early failure caused by debonding.
3) When width of CFRP is wider than the width of the RC beam, concrete cover separation occurs along the location of reinforcing steel bars because of the high

interfacial stresses between the concrete and the FRPs. Compared to wide CFRPs, U shaped straps are more effective to increase load capacity of the RC beams strengthened with FRPs by preventing early failure of RC beams arising from debonding.

References

[1] Gartner A, Douglas EP, Dolan CW, Hamilton HR, "Small beam bond test method for CFRP composites applied to concrete", Journal of Composites for Construction, 15(1), 52-61, 2010.

[2] Chataigner S, Caron JF., Benzarti K, Quiertant M, Aubagnac C, "Use of single lap shear test to characterize composite-to-concrete or composite-to-steel bonded interfaces", Construction and Building Materials, 25(2), 468-478, 2011.

[3] Sharma S. "Plate–concrete interfacial bond strength of FRP and metallic plated concrete specimens", Composites Part B: Engineering, 37(1), 54-63, 2006.

[4] ABAQUS Theory manual, User manual, Example Manual, Version 6.10. Providence, RI, 2010.

[5] J. Yang, J. Ye, "An improved closed-form solution to interfacial stresses in plated beams using a two-stage approach", International Journal of Mechanical Sciences, 52(1): 13-30, 2010.

[6] J. G. Teng, J. F. Chen, S.T. Smith, L. Lam, "FRP retrofitted RC structures", John Wiley & Sons, Inc, 2001.

[7] Q. Yang, Q. Qin, D. Zheng, "Analytical and numerical investigation of interfacial stresses of FRP–concrete hybrid structure", Composite Structures, 57(1-4), 221-226, 2002.

[8] S. Smith, J. G. Teng, "FRP-retrofitted RC beams I: review of debonding strength models", Engineering Structures, 24(4), 385-395, 2002.

[9] Smith S, Teng JG, "FRP-retrofitted RC beams II: assessment of debonding strength models", Engineering Structures , 24(4), 397-417, 2002.

[10] Kamel AS, Elwi AE, Cheng RJ, "Bond model for FRP sheets bonded to concrete. Emirates Journal for Engineering Research", 9(2), 77-82, 2004.

[11] Teng JG, Yuan H, Chen JF, "FRP-to-concrete interfaces between two adjacent cracks: Theoretical model for debonding failure", International Journal of Solids and Structures, 43(18-19), 5750-5778, 2006.

[12] Teng JG, Yao J. "Plate end debonding failures of FRP- or steel-plated RC beams: A new strength model. In: Proceedings of the International Symposium on Bond Behaviour of FRP in Structures, BBFS 2005, 283-290, 2005.

[13] Utui N, "A study on the bonding performance of hybrid fiber reinforced polymers (FRPs)", Master's degree thesis, Ewha Womans University, Seoul, South Korea, 2011.

[14] Kim HS, Shin YS. "Flexural behavior of RC (RC) beams retrofitted with hybrid fiber reinforced polymers (FRPs) under sustaining loads", Composite Structures, 93(2), 802-811, 2011.